C. Strąk, W. Olesińska, R. Siedlec

Influence of carbon and oxygen on properties of Cu-C-O composites

Cezary Strąk, Wiesława Olesińska, Robert Siedlec

Instytut Technologii Materiałów Elektronicznych

ul. Wólczyńska 133, 01 - 919 Warszawa

e-mail: cezary.strak@itme.edu.pl

Abstract: The basis od this project was to produce volumetric composites using copper, copper oxide as well as commercial graphene powders and thermally reduced graphene oxide, on which copper oxide (CuO) was deposited by electrochemical bath. The graphene powders were annealed in an oxygen-free atmosphere and underwent Spark Plasma Sintering. The outcome composites were first copper-plated and then using silver solders (AG-Sn) welded to corundum ceramics. We examined the microstructure, physical and thermal properties of the composite itself and also the microstructure and flexural strength of the obtained joints. These studies helped us indicate the effect of carbon and oxygen on the changes of the thermal expansion coefficient in Cu-C-O composites.

Key words: thermal expansion coefficient, bonding, composite, carbon, oxygen, SPS

Wpływ grafenu i tlenu na właściwości kompozytów miedź-tlen-węgiel

Streszczenie: Kompozyty objętościowe wykonano stosując proszki miedzi, tlenku miedzi oraz handlowego grafenu i zredukowanego termicznie tlenku grafenu, na których osadzano tlenek miedzi metodą strącania z kąpieli elektrochemicznej. Proszki grafenu poddano obróbce termicznej w atmosferze beztlenowej, a następnie spieczono z nich kształtki stosując technikę SPS (*Spark Plasma Sintering*). Uzyskane kompozyty spajano z ceramiką korundową za pomocą lutów srebrowych (Ag-Sn). Przed procesem spajania kompozyty poddano procesowi galwanizacji miedzią. Zbadano mikrostrukturę, właściwości fizyczne i cieplne samego kompozytu oraz mikrostrukturę i wytrzymałość uzyskanych złączy. Na podstawie przeprowadzonych badań określono wpływ węgla i tlenu na zmiany współczynnika rozszerzalności cieplnej kompozytów Cu-C-O.

Słowa kluczowe: współczynnik rozszerzalności cieplnej, spajanie, kompozyt, węgiel, tlen, SPS

1. Introduction

For many years, there has been a growing interest in composite materials a they show properties, often superior to those of conventional materials and open up a whole range of possibilities to choose from such as the type of constituent phases, their form, quantity, distribution, probable orientations as well as their production method. Based on a dependence referred to as the rule of mixtures, the properties and amount of the reinforcing phase exert influence, among others, on density, thermal expansion and the coefficient of elasticity. A precondition for producing composites with optimal properties is to obtain an excellent matrix-reinforcing phase adhesion. This in turn inextricably requires satisfactory wettability of the surface of fibres (particles) and a lack of bubbles and voids, the conditions crucially depending on the production method of a composite. In addition, the characteristics of composites are to a high extent conditioned by both inter-particle spacing and inter-fiber distance. Changing these distances is likely to result in the presence of high local stress and zones of compressive stress. The reinforcement-matrix interface is probably the most crucial characteristic of composites. It has a direct effect on the quality of the reinforcement-matrix in particular coupling, vibration damping, the cracking mechanism of a composite as a whole and the inter-crystalline cracking of the matrix itself. The chemical and phase composition of the outcome coupling between components is of a great importance to mechanical properties and corrosion resistance contributing to the premature destruction of the material [1 - 2].

The development of a joining technology for graphene-reinforced composites and classical materials will broaden the range of their application. These joints should show a very high thermal conductivity and a relatively low thermal expansion coefficient. There is a demand for materials dissipating heat from electronic systems in an efficient manner, especially those which are high-power and do not generate their thermal residual stresses. Only composite materials can meet such requirements and scientific studies point out two composites, Cu-C and Cu-Cu$_2$O [2 - 3].

Thermal expansion is one of the basic physical properties of solids and gases, considerable practical, both positive and negative significance. This property entails increasing the volume of the solid body with temperature, while maintaining constant pressure. One of the consequences of different atomic bond energies in solids is their dissimilar susceptibility to size changes induced by temperature fluctuations. From a practical viewpoint, the quantitative description of the change of the dimensions of the solid is more important than the qualitative description. Linear and volumetric thermal expansion coefficients are used for this purpose. The former applies only to solids since the length parameter can be assigned only to them, whereas the latter characterizes the behaviour of all bodies

undergoing temperature-based size changes, irrespective of their physical state. Each of the thermal expansion coefficients provides information about how particular materials react to the same temperature change. It has to be remembered that the temperature change can result in a material shrinkage, which most often takes place during the cooling stage.ge. Therefore, the direction of the temperature change in a material determines the type of the changes of size. As a result, the thermal expansion coefficient can have either positive or negative values, depending on the said temperature change direction. For scientific exactitude, it has to be added that due to the measurement hysteresis the coefficient values obtained at the same temperature when heated and cooled are not identical.

The development of a new, copper-based joints which in industrial practice allows for copper direct bonding, is an ecological and energy saving technology which by using a Cu-Cu$_2$O eutectic mixture enables obtaining vacuum tight joints [4 - 7].

Previous research shows that addition of carbon helps maintain high thermal conductivity. With copper-carbon composite it must be remembered that the thermal expansion coefficient is a function of temperature. It also seems that equally good parameters can be obtained for the copper-copper oxide composite. Modification of copper by using its oxides gives a homogeneous material with properties different from these of pure copper. Combining high thermal conductivity with the regulated expansion coefficient will lead to the production of a unique material which could be used in heat sinks in electronics.

All composite-related technologies pose significant problems with appropriate wettability between the matrix and reinforcement phases and on the boundary between the bonded elements. In the case of the study presented in this paper, a major hindrance appears to be the non--wettability of carbon by liquid metals. In general, wetting phenomena play a detrimental role in all manufacturing processes of composites involving the presence of the liquid phase (of the matrix) [8 - 10].

Composites having a graphene reinforcement belong to a group of materials with a unique microstructure and excellent electrical, thermal and mechanical properties. The exceptional characteristics of graphene and fairly easy process of production of both polymer- and ceramics-based composites, facilitated their application in transparent conductors [11 - 12]. Despite all well-known technologies and a great variety of carbon-copper composites (with carbon fibres or graphite), the copper-graphene composites are still rather modestly described in the literature. The production of these composites is not without a great number of problems wchich apart from the already-mentioned non-wettability, result from the shape of graphene and its flake-based structure. The well-developed structure and a lack of continuity do not guarantee sukcess of graphene and the reinforcement material blending when solid phase components are mixed together [13].

The purpose of this research was to develop a production method of a Cu-C-O composite with the expansion coefficient lower than that for copper, while preserving high thermal conductivity, which could be used in elements dissipating heat from copper-ceramics systems, including dissipating heat generated during the operation of a laser. The use of carbon nanoparticles (graphite, dispersed graphene) and copper oxides (Cu$_2$O; CuO) gives a homogeneous material exhibiting anisotropic properties, suitable for combining it with materials of low linear expansion coefficient (corundum ceramic materials, nitrides or carbides). The thermal expansion coefficient values for these materials are as follows: Cu – around 18×10^{-6} K^{-1}, Cu$_2$O – 4.3×10^{-6} K^{-1}, CuO – 9.3×10^{-6} K^{-1} and C – $6,5 \times 10^{-6}$ K^{-1}. Our comparative study (examinations) of the properties of two chemically different types of composites, i.e. Cu-C and Cu-Cu$_2$O, was carried out together with weldability tests with corundum ceramics, which is an essential prerequisite for their application in heat-dissipating systems [14 - 15].

2. Starting materials

In order to produce volumetric composites, we used carbon in a form of thermally reduced graphene oxide (rGO) and commercially available graphene from an American company called Sky Spring Nanomaterials as well as Cu and Cu$_2$O powders from Aldrich Company. Copper oxide nanopowder was deposited onto graphene powders using the sol-gel method based on a liquid containing copper sulfate, sodium hydroxide, formaldehyde and potassium sodium tartrate. Next, the products were annealed at 600°C in a nitrogen atmosphere with oxygen content of around 1.5 ppm. This process transformed cupric oxide (CuO) into cuprous oxide (Cu$_2$O) without copper grains. The deposition process after the mixture of Cu$_2$O-15 wt. % rGO (or graphene from the USA) was obtained.

2.1. Thermally reduced graphene oxide (rGO)
The analysed material was developed in the Department of Chemical Technologies of ITME. A cluster of rGO flakes few micrometres in size, randomly arranged is presented in Fig. 1. The structure analysis of rGO was carried out using Carl Zeiss AURIGA CrossBeam scanning electron microscope. A side detector (SE) and an in-lens detector were employed to create SEM images, using detection of secondary ions at the accelerating voltage level of 0.46, 1; 5 and 20 kV.

The result of deposition of Cu on rGO flakes are shown in Fig. 2. Both, single grains and complex copper crystallites can be seen on the rGO flakes. The annealing process at 600°C caused a rounding of the Cu particles. After this process the change of material colour from black to brown was also observed with the naked eye.
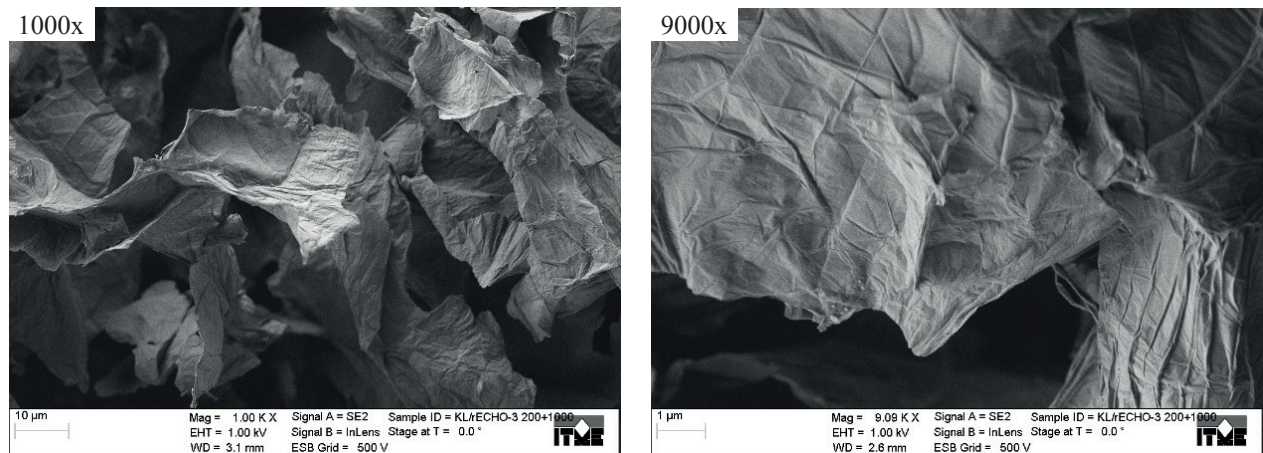
Fig. 1. SEM image of thermally reduced graphene oxide.
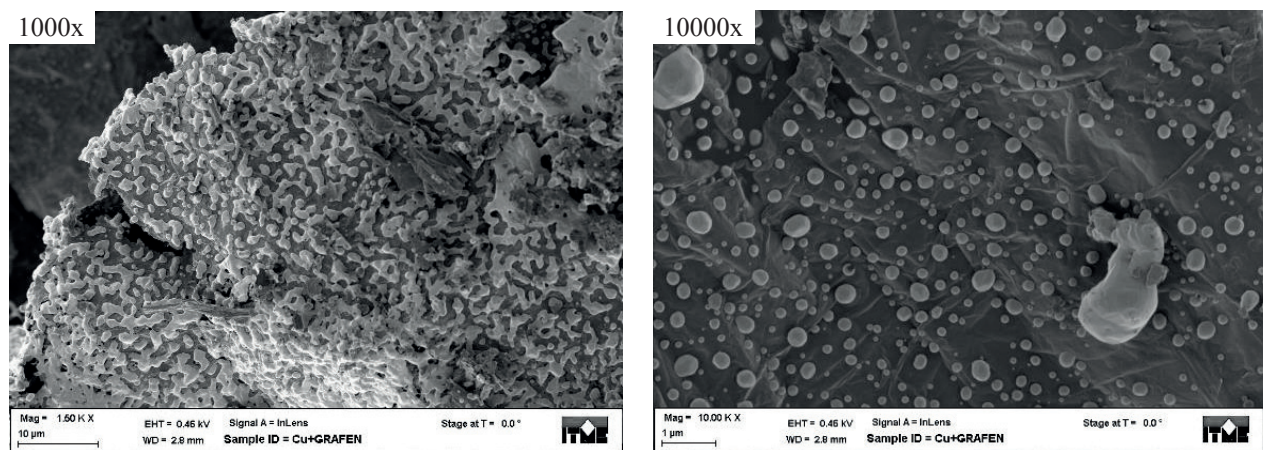**Rys. 1.** Obraz SEM rGO.

Fig. 2. SEM images of rGO covered with copper oxide, after annealing at 600°C.
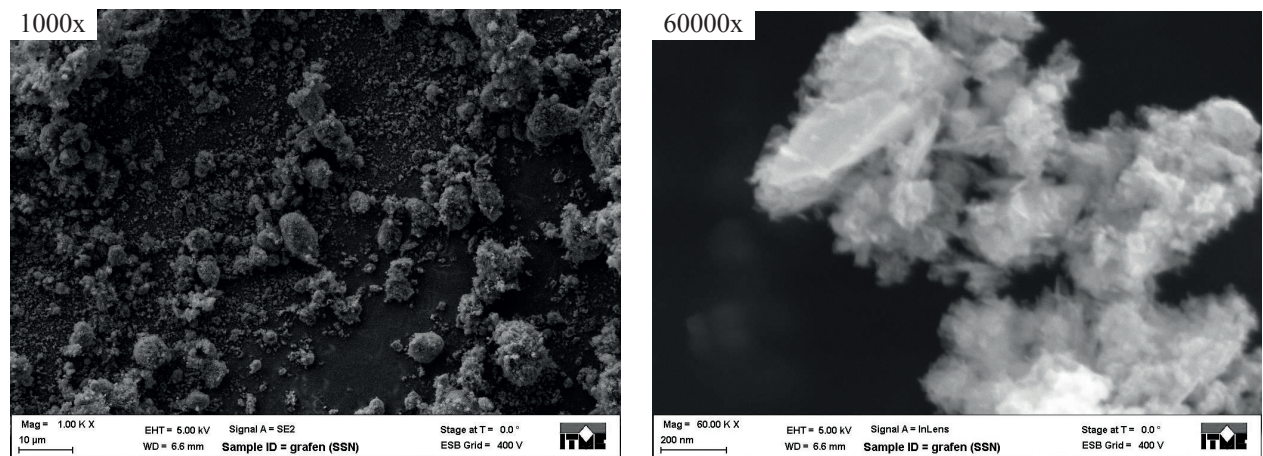**Rys. 2.** Obrazy SEM rGO pokrytego tlenkiem miedzi, wyżarzonego w temperaturze 600°C.

Fig. 3. SEM image of commercial graphene.
Rys. 3. Obraz SEM handlowego grafenu.

2.2. Commercial graphene (USA)

The microstructure of the analysed material is shown in Fig. 3, whereas Fig. 4 presents the same material after deposition of copper oxide. As it can be seen in Fig. 1, the morphology of commercial graphene is significantly different from the morphology of rGO. It is impossible to see a flake-based structure but rather very fine grains and agglomerates of diverse shapes. The precipitated particles of copper oxide were unevenly distributed in the material, forming clusters different in shapes and dimensions. No flake structures, typical for ITME rGO powders, were found.
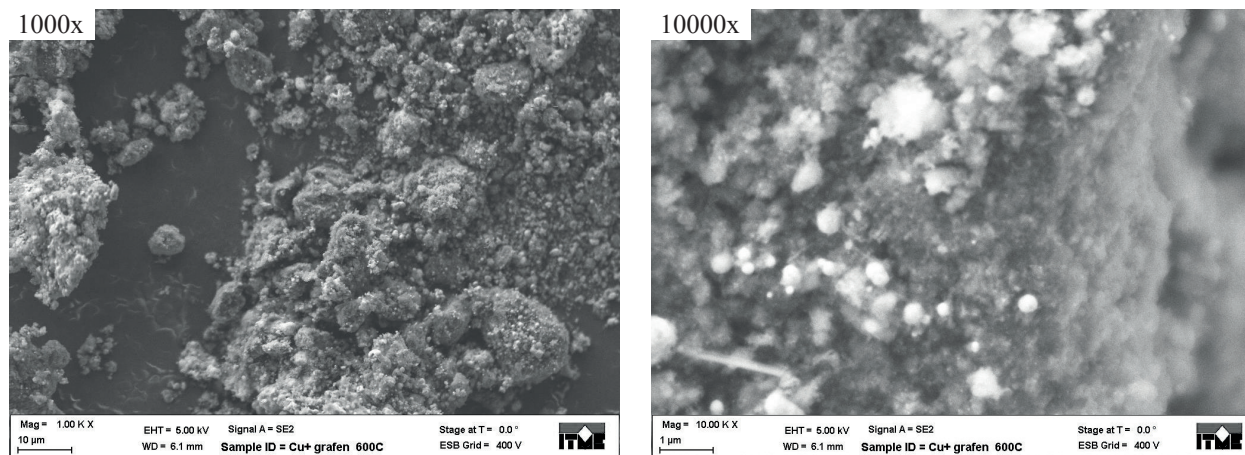
Fig. 4. SEM images of commercial graphene covered with copper oxide, after annealing at 600°C.
Rys. 4. Obrazy SEM handlowego grafenu pokrytego tlenkiem miedzi, wyżarzonego w temperaturze 600°C.
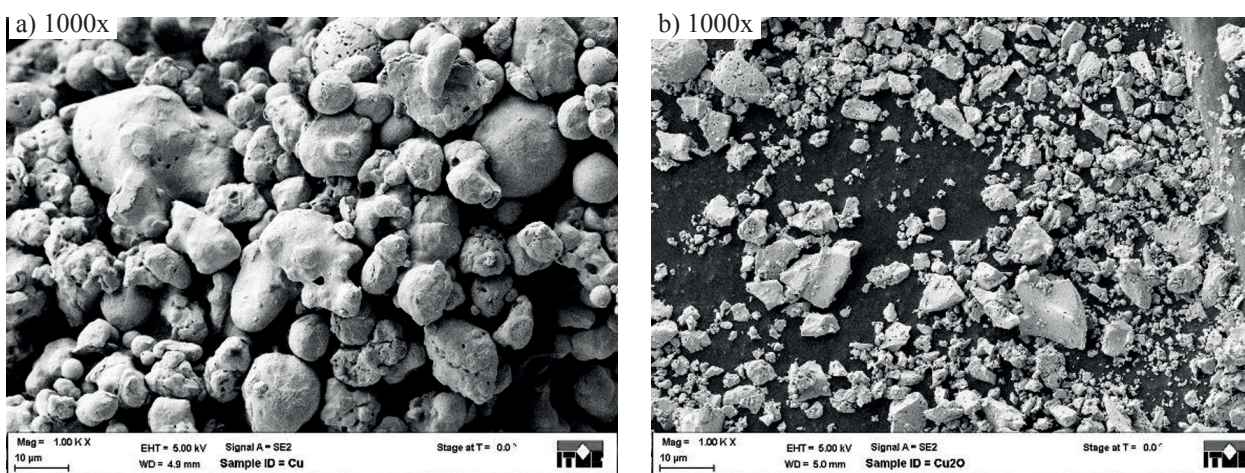

Fig. 5. SEM images of: a) ductile copper and b) copper oxide (I) powders.
Rys. 5. Obrazy SEM proszków: a) miedzi sferoidalnej, b) tlenku miedzi (I).

Similar to process for rGO ITME the reduction reaction and a change of colour of powder material from black to brown was observed after the annealing.

2.3. Copper and copper oxide

Another material investigated in this study was copper. We used ductile copper powder with the purity of 99% and the particle size in the range of $1 \div 40$ μm (Fig. 5a) from Aldrich Corporation and polyhedral copper oxide made by Aldrich Corporation with purity of 97% and the particle size in the $0.5 \div 15$ μm range (Fig. 5b).

3. Composites production

The production of composites was performed with the use of the above mentioned starting materials. Powder mixtures were sintered using a spark plasma sintering (SPS) system in the following conditions: the temperature of 950°C, pressure of 50 MPa, time of 15 min. Three types of composites were sintered in each instance with two different weight percentage compositions:

1. 80% Cu – 20% (Cu$_2$O – 15% rGO)
   and 85% Cu – 15% (Cu$_2$O –15% rGO),
2. 80% Cu – 20% (Cu$_2$O – 15% graphene from the USA)
   and 85% Cu – 15% (Cu$_2$O – 15% graphene USA),
3. 80% Cu – 20% Cu$_2$O and 85% Cu – 15% Cu$_2$O.

The rGO-based composites are characterized by the occurrence of elongated graphene forms, quite evenly distributed in the copper matrix (Fig. 6 - 7). Such an oblong character of the graphene forms results from the flake structure of rGO, whereas the layered structure is connected with the pressing direction.

In the case of the composites containing USA graphene, both fine graphene inclusions and large agglomerates, unevenly distributed in the copper matrix, could be observed (Fig. 8 - 9). Neither elongated inclusions, nor layered structure appeared in these composites. In addition, the direction in which a sample was pressed remained unnoticed.

The composites with copper oxide, showed a homogeneous structure (Fig. 10 - 11), without any layers, irrespective of the number of the components in the mixture.
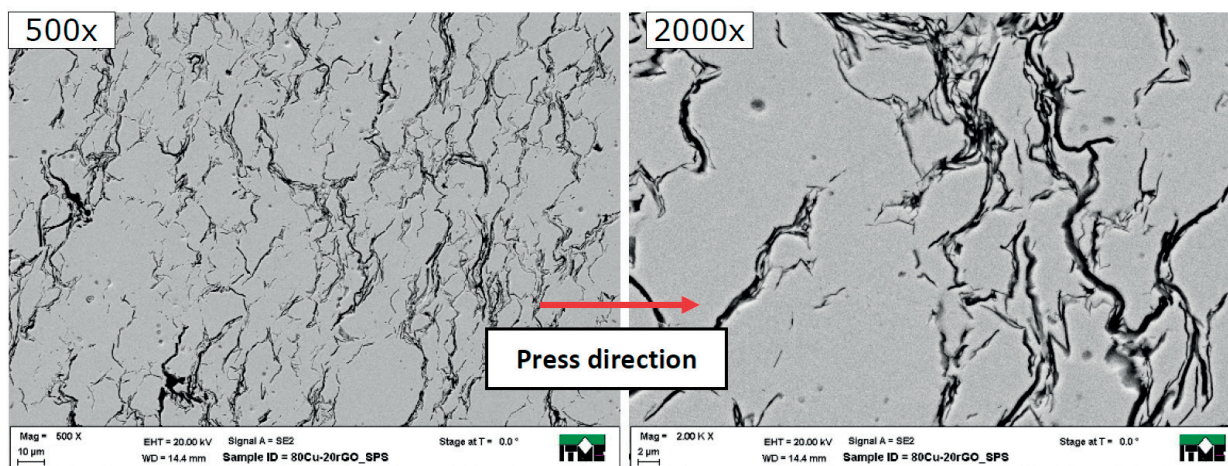
Fig. 6. SEM images of the 80% Cu - 20% (Cu_2O-15% rGO) composite.
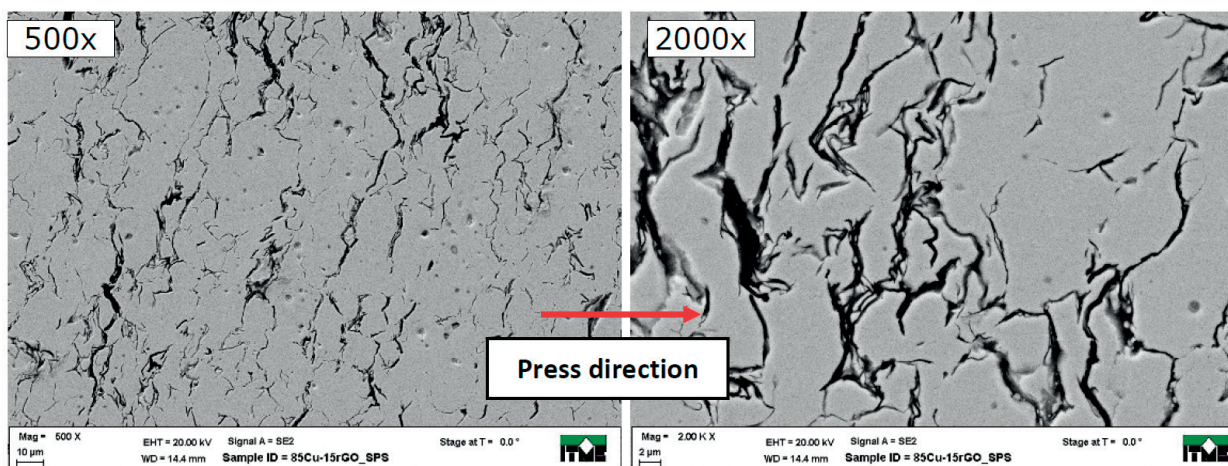**Rys. 6.** Obrazy SEM kompozytu 80% Cu – 20% (Cu_2O-15% rGO).

Fig. 7. SEM images of the 85% Cu – 15% (Cu_2O - 15% rGO) composite.
Rys. 7. Obrazy SEM kompozytu 85% Cu – 15% (Cu_2O - 15% rGO).
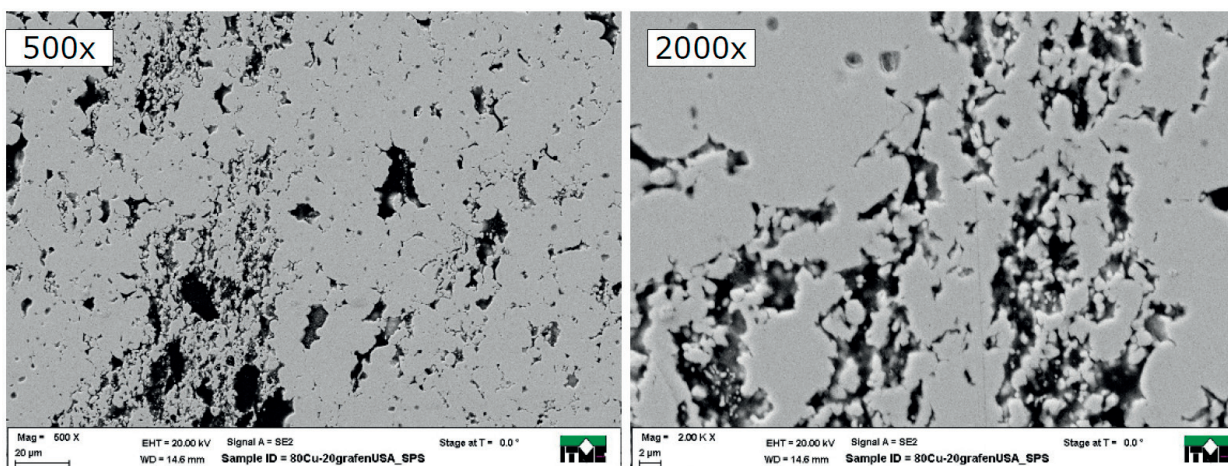

Fig. 8. SEM images of the 80% Cu – 20% (Cu_2O - 15% graphene from the USA) composite.
Rys. 8. Obrazy SEM kompozytu 80% Cu – 20% (Cu_2O - 15% grafen USA).

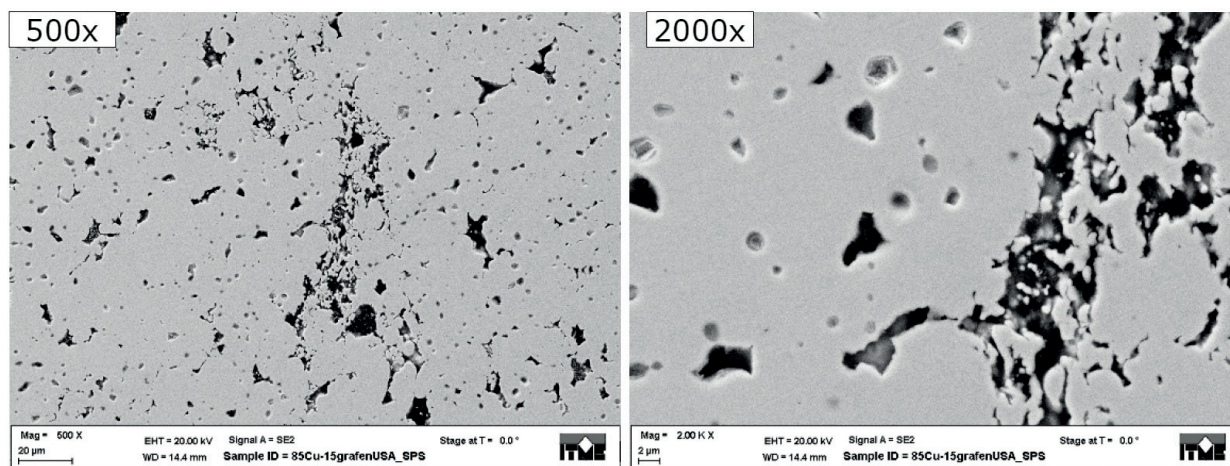**Fig. 9.** SEM images of the 85% Cu – 15% (Cu$_2$O – 15% graphene from the USA) composite.
Rys. 9. Obrazy SEM kompozytu 85% Cu – 15% (Cu$_2$O – 15% grafen USA).
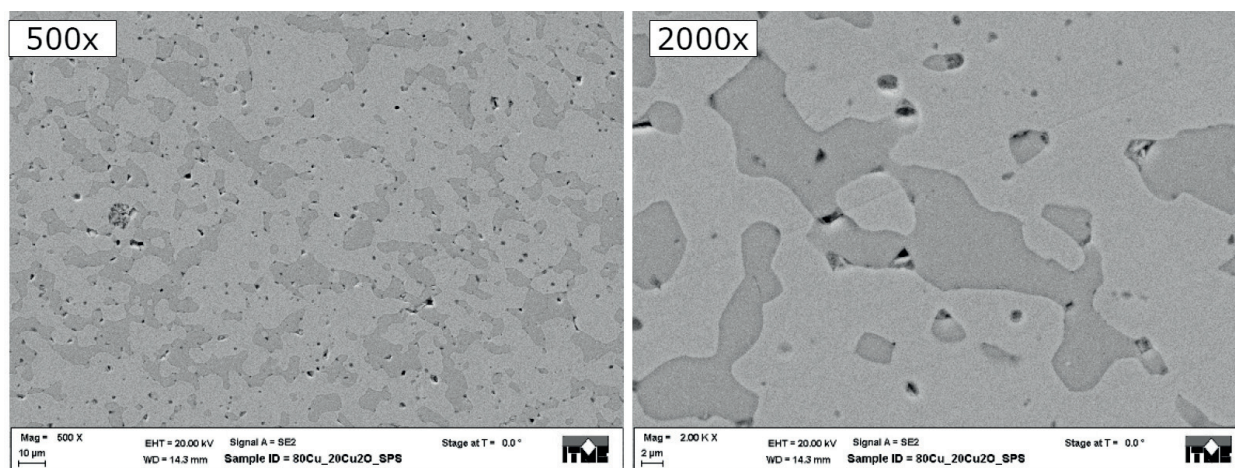

Fig. 10. SEM images of the 80% Cu – 20% Cu$_2$O composite.
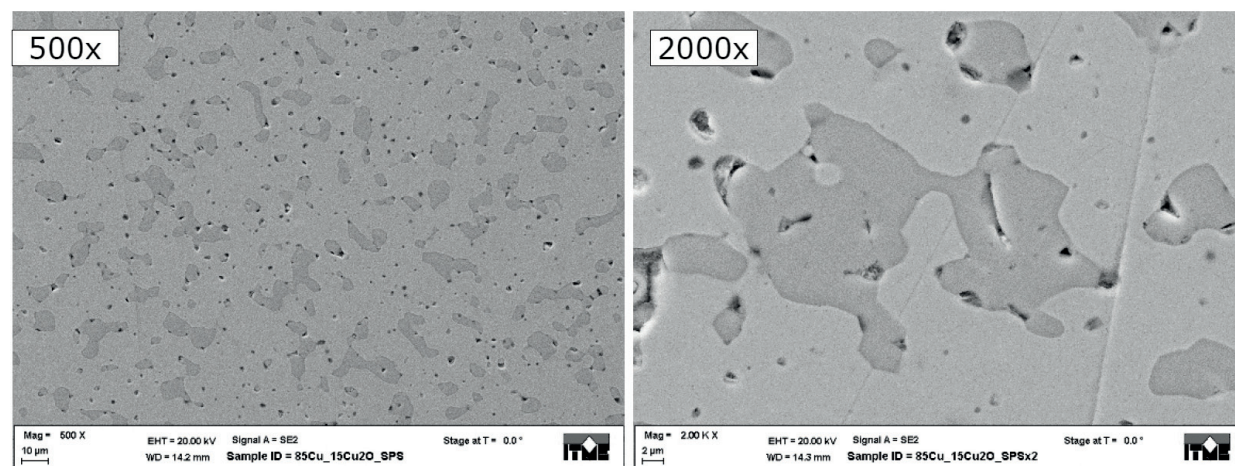**Rys. 10.** Obrazy SEM kompozytu 80% Cu – 20% Cu$_2$O.

Fig. 11. SEM images of the 85% Cu – 15% Cu$_2$O composite.
Rys. 11. Obrazy SEM kompozytu 85% Cu – 15% Cu$_2$O.

Darker copper oxide grains were evenly distributed in the copper matrix. In the case of all composites, pores were present in the structure.

4. Properties of composites

In the course of our research density was measured by a hydrostatic balance based on the Archimedes law. The measurements of hardness were performed by way of Vickers technique, with Struers Dura Scan 10 System and the load of 100 g. The highest hardness was noted for copper sintered following the SPS method.

The analysis of composites showed the highest hardness rate for sinters with an addition of copper oxide and the lowest values for sinters with graphene from the USA. A similar tendency is observed for the entire range of composites. Those containing components with 80 - 20 weight ratio are harder than those obtained using the 85 - 15 weight ratio (Tab. 1).

Thermal conductivity was measured by a pulsed laser method using the NETZSCH LFA 457 equipment. The value obtained for the composites is significantly lower than the theoretical conductivity of copper (400 W/mK) and lower than in the case of the copper sinter produced using the SPS technique (around 390 W/mK – see Tab. 2). This difference in the obtained values results from the occurence of porosity, which substantially lowers thermal conductivity. Gases present in pores are a direct consequence of co-precipitation of copper oxide on graphene powder. Despite the reduction of powder at 600°C in a nitrogen atmosphere (with oxygen content of around 1.5 ppm) and the sintering process in vacuum, a significant amount of oxygen can still be found in the material.

The thermal conductivity measurement results for particular composites show that the higher values are obtained in the case of composites with 15% of carbon dopant. This means that when the fraction of the reinforcing phase is increased, thermal conductivity gets lower. The highest

Tab. 1. Value of density and hardness of composites [g/cm³].
Tab. 1. Gęstość i twardość kompozytów [g/cm³].

Material	Density [g/cm³]	Relative density [%]	Theoretical density [g/cm³]	Hardness [HV0.1]
80% Cu – 20% Cu₂O	7.91	94.5	8.37	78.8
85% Cu – 15% Cu₂O	8.07	94.7	8.52	67.7
80% Cu – 20% (Cu₂O - 15% rGO)	7.99	97.5	8.194	69.3
85% Cu – 15% (Cu₂O - 15% rGO)	8.17	97.4	8.386	64.1
80% Cu – 20% (Cu₂O - 15% graphene USA)	7.63	92.8	8.224	56.3
85% Cu – 15% (Cu₂O - 15% graphene USA)	7.79	92.6	8.408	55.6
Cu sintered using SPS	8.77	97.9	8.96	109

Tab. 2. Thermal conductivity of composites and σ deviation [W/mK].
Tab. 2. Przewodność cieplna kompozytów i odchylenie standardowe [W/mK].

| Temperature [°C] | Thermal conductivity [W/mK] | | | | | | | | | | | |
| | 50 | | 100 | | 150 | | 200 | | 250 | | 300 | |
	wart.	σ	wart.	σ	wart.	σ	wart.	σ	wart.	σ	wart.	σ
80% Cu – 20% Cu₂O	198.4	11.7	193.6	1.1	188.2	1.8	184.7	3.6	182.6	1.2	177.7	2.1
85% Cu – 15% Cu₂O	257	4.4	250.6	1.2	247.2	0.9	245.5	1.9	240.1	0.7	238.2	2.3
80% Cu – 20% (Cu₂O – 15% rGO)	119.4	4.1	116.4	1.1	115.6	0.4	110.6	0.8	112.1	0.7	109.1	1.4
85% Cu – 15% (Cu₂O – 15% rGO)	156.7	4.6	163.8	1.9	161.8	0.5	159.3	1.8	157.6	2.9	156.1	2.1
80% Cu – 20% (Cu₂O – 15% g USA)	185	8.7	186.6	3.5	182.5	0.4	180.6	2.1	177.9	2.3	176	1.9
85% Cu – 15% (Cu₂O – 15% g USA)	234.6	6	230.5	1.6	230.7	1.3	228.3	2	226.9	1.3	222.4	6.4
Pure Cu sintered using SPS	390.4	21.0	383.4	6.3	380.0	2.1	375.2	2.1	371.7	1.8	366.8	1.5
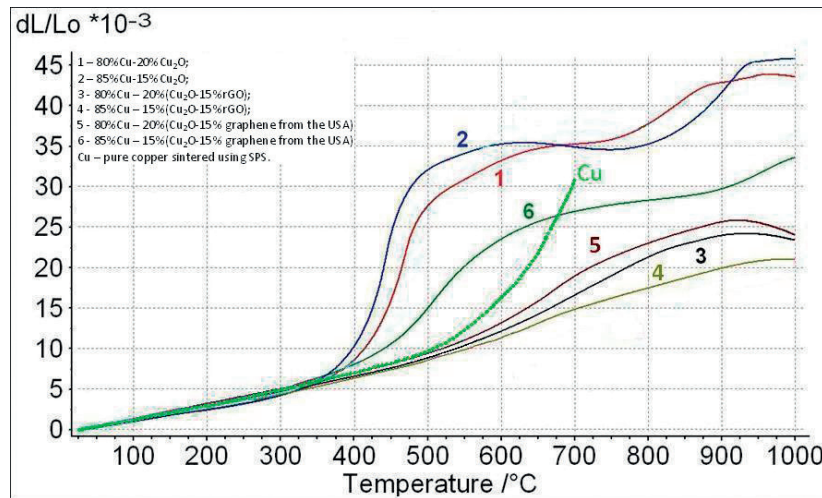
Fig. 12. Relation between elongation and temperature: 1 – 80% Cu – 20% Cu₂O; 2 – 85% Cu – 15% Cu₂O; 3 - 80% Cu – 20% (Cu₂O – 15% rGO); 4 – 85% Cu – 15% (Cu₂O-15% rGO); 5 – 80% Cu – 20% (Cu₂O – 15% graphene from the USA); 6 – 85% Cu – 15% (Cu₂O – 15% graphene from the USA); Cu – pure copper sintered using SPS.

Rys. 12. Wykres zależności wydłużenia od temperatury: 1 – 80 % Cu – 20% Cu₂O; 2 – 85% Cu – 15% Cu₂O; 3 – 80% Cu – 20% (Cu₂O – 15% rGO); 4 – 85% Cu – 15% (Cu₂O – 15% rGO; 5 – 80% Cu – 20% (Cu₂O – 15% grafen USA); 6 – 85% Cu – 15% (Cu₂O – 15% grafen USA); Cu spieczona techniką SPS.
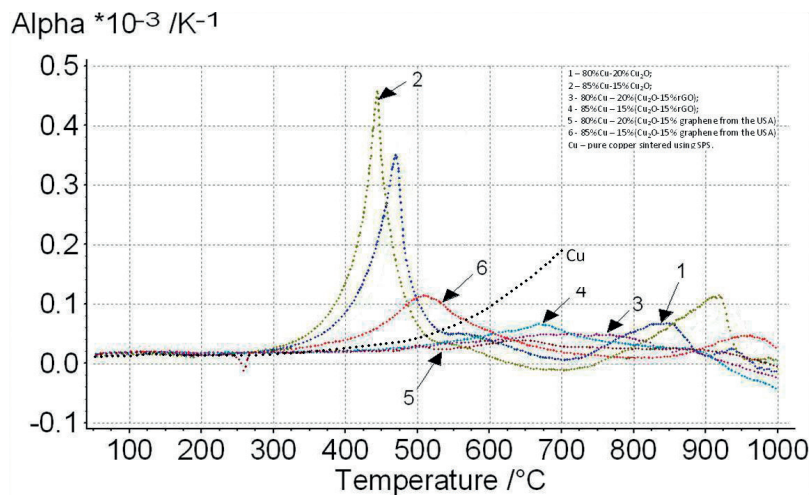
Fig. 13. Relation between Alpha thermal expansion coefficient and temperature: 1 – 80% Cu – 20% Cu₂O; 2 – 85% Cu – 15% Cu₂O; 3 – 80% Cu – 20% (Cu₂O – 15% rGO); 4 – 85% Cu – 15% (Cu₂O – 15% rGO; 5 – 80% Cu – 20% (Cu₂O – 15% graphene from the USA); 6 – 85% Cu – 15% (Cu₂O – 15% graphene from the USA); Cu – pure copper sintered using SPS.

Rys. 13. Wykres zależności współczynnika rozszerzalności cieplnej Alpha od temperatury: 1 – 80% Cu – 20% Cu₂O; 2 – 85% Cu – 15% Cu₂O; 3 – 80% Cu – 20% (Cu₂O – 15% rGO); 4 – 85% Cu – 15% (Cu₂O – 15% rGO; 5 – 80% Cu – 20% (Cu₂O – 15% grafen USA); 6 – 85% Cu – 15% (Cu₂O – 15% grafen USA); Cu spieczona techniką SPS.

thermal conductivity was reached for composites with both USA graphene and Cu₂O.

Thermal expansion coefficient was analysed at the same time with the help of a NETZSCH DIL 402C/4/G dilatometer. The results are collected in Fig. 12 - 13.

The investigated samples 1 and 2 show higher dilatation than the Cu sample which is confirmed by a rapid increase in length. The observed process starts at the temperature of around 300 – 400°C. This applies mainly to oxide-reinforced composites and is least visible in the case of graphene-reinforced composites. The smallest elongation, at the same time bearing the closest resemblance to copper, is observed for the composites reinforced with

rGO. In the temperature range between the ambient temperature and 350°C there is a constant value of the thermal expansion coefficient and a steady growth of elongation in the case of all investigated samples. Starting from the temperature of approximately 400°C and up to around 500°C there is a sharp rise in the alpha coefficient and the elongation of the composites reinforced with Cu₂O.

The properties of composite mixtures containing Cu and Cu₂O and the same ones with an addition of the graphene from the USA are unstable and at 300 – 450°C undergo transformations causing less abrupt size changes than in the case of the oxide composite. Further heating of all analysed composites at 500 – 800°C causes a simi-

lar length increase and the expansion changes are in the – 0.02 – 0,05·10⁻³/K⁻¹ range.

The expansion coefficient in the investigated temperature range for samples made of the same powders and sintered in identical conditions using the SPS method ranges between – 0.02 × 10⁻³ and 0.2 × 10⁻³K⁻¹. The most significant decrease in the coefficient value and the most repeatable changes are observed for the Cu–Cu$_2$O–C composites. Dilatometric modifications of the Cu–Cu$_2$O composites, most probably linked with the high amount of gases, can exert a destructive influence on the properties of the welded joints in the 350 – 450°C range. Much lower thermal expansion coefficient and lower length than in the case of copper can be observed for graohene-reinforced composites, sintered at temp. exceeding 500°C.

5. Joining of Cu–O–C composites

The objective of this study was to prepare joints so that their microstructure could be investigated by conducting analysis on their cross-sections. The joining process of the composites took place in a tunnel furnace in both neutral and reducing atmospheres. Composites were soldered to corundum ceramics at the temperature of 400°C in a nitrogen atmosphere using the S-Sn97Ag3 solder. Before the joining process, the produced composites were subjected to a galvanic deposition of a copper layer (according to Fig. 15 – 17 the thickness of this layer was 5 um) which activated and homogenized the surface of the composite to improve its wettability by the solder. Corundum ceramics, before the joining process underwent galvanic deposition of a nickel layer or corundum ceramics with a sintered layer of MoMn covered with Ni.

● **Joint 1.** The 80% Cu – 20% Cu$_2$O composite covered with a layer of copper – corundum ceramics covered with a layer of electrochemical nickel (Fig. 14).
● **Joint 2.** The 85% Cu – 15% (Cu$_2$O – 15% rGO) composite covered with a layer of copper – corundum ceramics with a sintered layer of MoMn covered with Ni (Fig. 15).
● **Joint 3.** The 85% Cu – 15% (Cu$_2$O – 15% graphene from the USA) composite covered with a layer of copper – corundum ceramics with a sintered metallic layer of MoMn covered with Ni (Fig. 16).
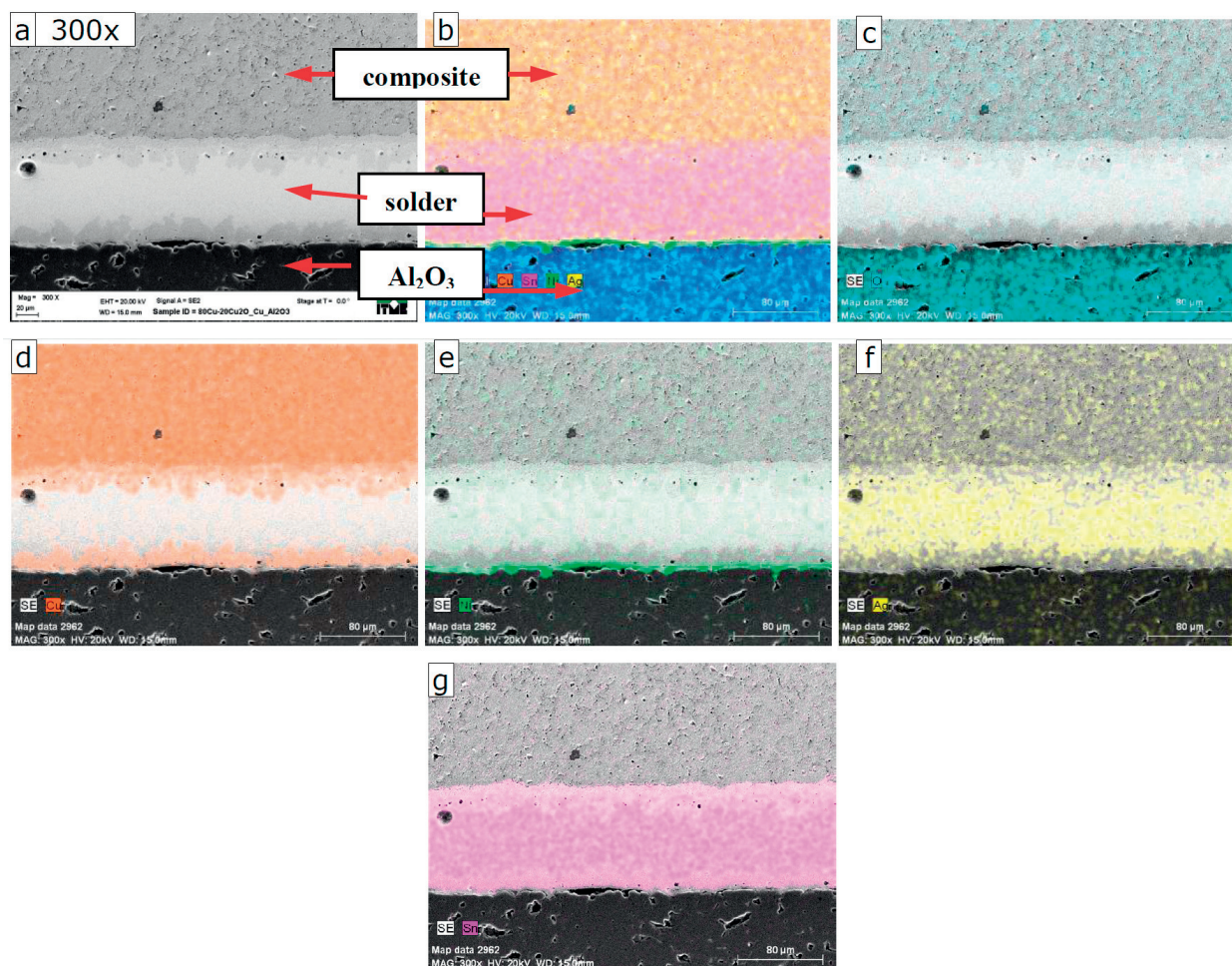

Fig. 14. Distribution map of chemical elements over the cross section of joint 1: a) SEM image, b) O, Al, Cu, Sn, Ni and Ag maps, c) O map, d) Cu, e) Ni, f) Ag, g) Sn.
Rys. 14. Mapy rozkładu pierwiastków na przekroju złącza 1: a) obraz SEM; b) mapa O, Al, Cu, Sn, Ni, Ag; c) mapa O; d) Cu; e) Ni; f) Ag, g) Sn.

Fig. 15. Distribution map of chemical elements over the cross section of joint 1: a) SEM image, b) C, O, Al, Cu, Sn, Ag, Ni, Mo and Mn maps, c) C map, d) O, e) Cu, f) Ag, g) Sn, h) Mo, i) Mn.
Rys. 15. Mapy rozkładu pierwiastków na przekroju złącza 1: a) obraz SEM; b) mapa C, O, Al, Cu, Sn, Ag, Ni, Mo, Mn; c) mapa C; d) O; e) Cu; f) Ag; g) Sn; h) Mo; i) Mn.

Fig. 16. Distribution maps of chemical elements over the cross section of joint 3: a) SEM image, b) C, O, Al, Cu, Sn, Ag, Mo, Mn and Ni maps, c) C map, d) O, e) Cu, f) Mo, g) Sn, h) Ag.
Rys. 16. Mapy rozkładu pierwiastków na przekroju złącza 3: a) obraz SEM; b) mapa C, O, Al, Cu, Sn, Ag, Mo, Mn, Ni; c) mapa C; d) O; e) Cu; f) Mo; g) Sn; h) Ag.

After the analysis of the particular joints (Fig. 14) , we can notice very good wettability of the surface of the composite and ceramics with a layer of nickel. Copper is diffused from the composite to the layer of the solder and metalization layer as seen in Fig. 14 and metalization layer seen in Fig. 15 and 16. Insignificant porosity can be observed in the layer of the solder from the side of the composite (Fig. 14 and 15). This effect can be related to the excess of oxygen which escapes from the composite to the atmosphere through the layer of the solder, thereby oxidating silver. Silver oxide is not wetted by the solder components and the reduced crystallites surrounded by the remaining components are accumulated, forming agglomerates (Fig. 16b). At around 200°C silver oxide is dissociated, whereas the escaping oxygen reveals large pores in the layer on the border between the solder and the composite. Complex graphene-containing agglomerates migrate to the top layers of the joined materials. Pores can be noticed in the boundary layers (border between

solder-composite and ceramic-solder), which proves the presence of a gaseous phase in a given composite (Fig. 15). Significantly fewer complex graphene forms are released to the surface in the case of joint 3 (Fig. 16).

SEM images performed on cross-section of the etched-joints (see Fig. 17) present a transition zone between the solder and the composite, with graphene agglomerates suspended in copper. Nickel, which is a component of the layers deposited onto ceramics during the welding process, migrates into the solder and towards the surface of the composite. In addition, the migration of silver crystals present in the solder was observed. Silver and nickel migrate to the grain boundaries of copper which is present in the composite. On the other hand, copper, which is both the matrix of the composite and the layer deposited onto the composite, is diffused to the tin-silver solder and the layer of nickel covering corundum ceramics. The compound forms of graphene, copper and oxygen remain in the layer of the composite. Oxygen was also identified in
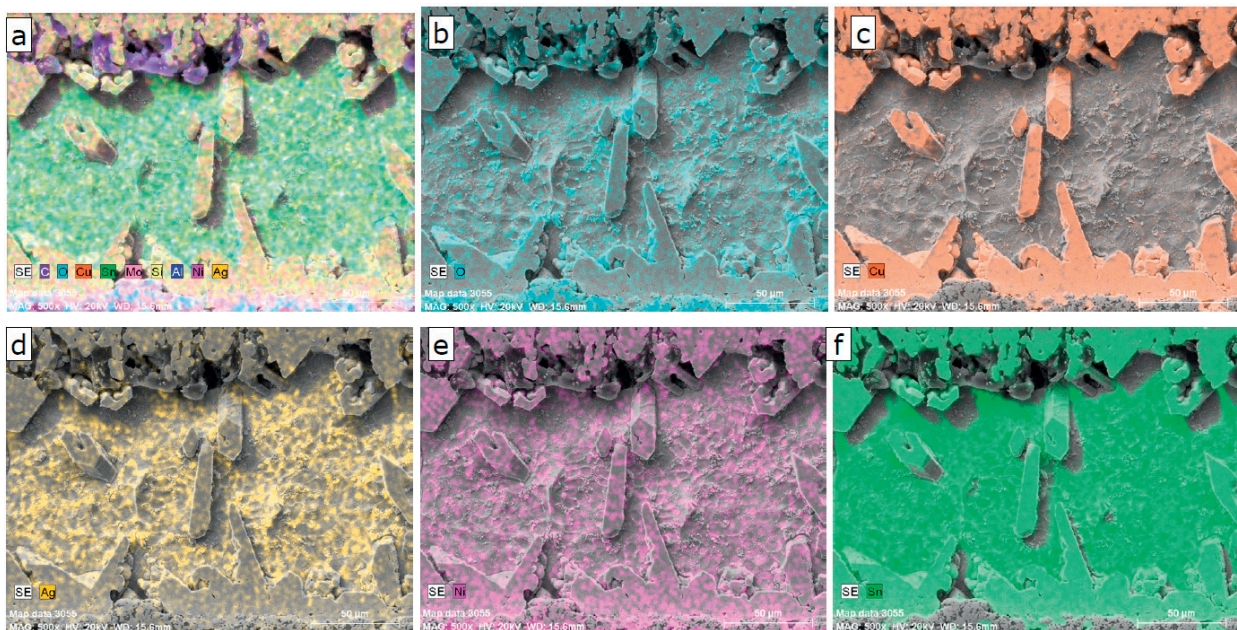

Fig. 17. Distribution maps of chemical elements over the 80% Cu – 20% (Cu_2O – 15% rGO) joint after etching in H_2O – HNO_3 solution in a ratio of 1:1, a) C, O, Al, Cu, Sn, Ag, Mo, Si and Ni maps, b) O map, c) Cu, d) Ag, e) Ni, f) Sn.
Rys. 17. Mapa rozkładu pierwiastków w złączu 80% Cu – 20% (Cu_2O – 15% rGO) po trawieniu w roztworze H_2O – HNO_3 w stosunku 1:1, a) C, O, Al, Cu, Sn, Ag, Mo, Si i Ni, b) O, c) Cu, d) Ag, e) Ni, f) Sn.
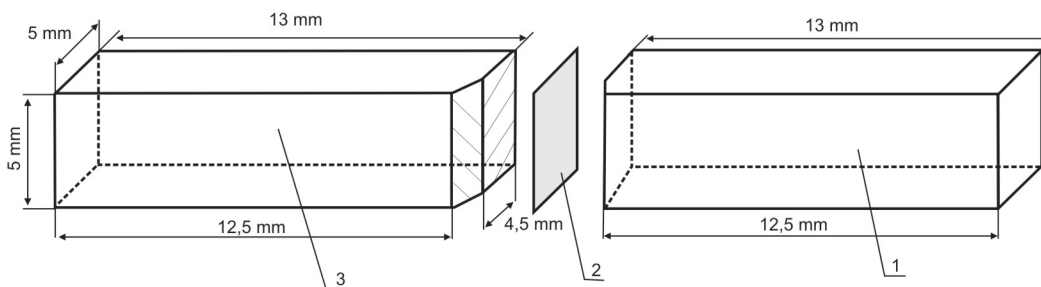

Fig. 18. A diagram of joints used in bending tests. 1 – composite, 2 – solder, 3 - Al_2O_3.
Rys. 18. Schemat wykonania złączy na zginanie. 1 - kompozyt, 2 - lut, 3 – Al_2O_3.

Tab. 3. Flexural strength of joints: composite – corundum ceramics.
Tab. 3. Wytrzymałość na zginanie złączy: kompozyt – ceramika korundowa.

Nr	Flexural strength σ_c [MPa]		
	85 Cu – 15Cu$_2$O	85% Cu – 15% (Cu$_2$O - 15% rGO)	85% Cu – 15% (Cu$_2$O – 15% graphene USA)
Avg.	42.4	42.6	41.7
σ	2.6	2.4	4.2

the structure of all composites. Attention must be paid to slight porosity in the transition zone (Fig. 15 - 16), caused by the diffusion of gases from the composite.

The investigation of the flexural strength σ_c (three--point bending) of composite-corundum ceramics joints (samples measuring 5 x 5 x 13 mm shown in Fig. 18) was carried out at a room temperature using a ZWICK 1446 testing machine equipped with a 1 kN head with the support spacing of 20 mm and the positioning speed of the head reaching 1.0 mm/min. Ceramic samples with the front part covered with Ni layers were applied during the welding process.

The mechanical flexural strength of joints is equal to strength R_m for the used SnAg3 solder (Tab. 3). The achieved values are repeatable, although a small deviation can be observed. One of the explanations of this fact can refer to a high quality of couplings and a low level of thermal stress in a joint. A continuous transition zone, consistent with the joined materials rich in metallic components of the solder and the composite is created in all joints. When bent, all the joints exhibited plastic deformation, without intense cracking. Fracture took place throught the layer of the solder.

6. Summary

This research project involves developing new Cu–Cu$_2$O, Cu–Cu$_2$O–rGO and Cu–Cu$_2$O–graphene USA composites. Cu–Cu$_2$O–graphene USA and Cu–Cu$_2$O–rGO composites are characterized by significantly lower linear thermal expansion than copper, and therefore can be used in a sintering process with corundum ceramics. At the temperature of 350 – 450°C, the composites containing 15% and 20% of the Cu$_2$O reinforcement probably show a oxide phase change, which can hinder their further use. Below this temperature range, the expansion coefficients of both copper and the composite did not differ significantly, whereas the above 500°C values for the composite were several times lower than the expansion coefficient of copper.

The rGO reinforcement of the Cu–Cu$_2$O composite brings a variety of changes to the properties of the materials, which was particularly advantageous to the joining process. First of all, the thermal expansion coefficient, several times lower than the expansion coefficient of copper, is stable for the 20 – 900°C temperature range.

Most probably, when the temperature rises rGO binds oxygen and limits phase changes in the composite. The composite with an addition of reduced graphene oxide lowers the hardness of copper, but does not minimize plastic deformation of the joints during the cooling process. The thermal conductivity of the composites remains lower than the thermal conductivity of copper sintered under the same conditions and shows a significant dependence on the type of the introduced graphene.

Acknowledgements

Literature

[1] Boczkowska A., Witemberg - Perzyk D., Kapuściński J., Puciłkowski K., Wojciechowski S., Lindemann Z.: Kompozyty, Wyd. Politechnika Warszawska, Warszawa, 2003

[2] Pietrzak K.: Formowanie się warstw pośrednich w kompozytach metalowo - ceramicznych i ich złączach, Oficyna Wydawnicza Politechniki Warszawskiej, Warszawa, 1998

[3] Shao W. Z., Feng L. C., Zeng L., Xie N.: Thermal expansion behavior of Cu0/Cu$_2$O cermetes with different Cu structures, *Ceramics International,* 2009, 35, 2803 - 2807

[4] Włosiński W., Olesińska W.: Spajanie kompozytów Cu-Cf z ceramiką korundową i stalą techniką CDB, Seminarium Kompozyty 1999: Teoria i Praktyka IV, Jaszowiec

[5] Kaliński D., Olesińska W., Chmielewski M., Pietrzak K.: Opracowanie nowej technologii wytwarzania próżnioszczelnych elementów elektroizolacyjnych ceramika-metal, Sprawozdanie z grantu, 2011, Nr N N 508 391 335

[6] Olesińska W., Kaliński D., Chmielewski M., Diduszko R., Włosiński W.: Influence of titanium on the

formation of a "barier" layer during joining on AIN ceramic with copper by the CDB technique., *J. Mater. Sci: Mater. Electron.,* 2006, 17, 781 - 788

[7] Pietrzak K., Olesińska W., Kaliński D., Strojny-Nędza A.: The relationship between microstructure and mechanical properities of directly Bondem copper-alumina ceramics joint, *Bulletin of the Polish Academy of Sciences, Technical Sciences*, 2014, 62, 1, 23 - 32

[8] Pietrzak K.: Nature and morphology of the interface layer in carbon fibre copper composites, The 4th European Conference and Advanced Materials and Processes, Padva/Venice, 1995, 463 - 467

[9] Barlak M., Piekoszewski J., Stanisławski J., Borkowska K., Sartowska B., Werner Z., Miśkiewicz M., Jagielski J., Starosta W.: The effect of titanium ion implantation into carbon ceramic on its wettability by liquid copper, *Vacuum,* 2007, 81, 1271 - 1274

[10] Barlak M., Piekoszewski J., Stanisławski J., Borkowska K., Sartowska B., Werner Z., Miśkiewicz M., Starosta W., Składnik - Sadowska E., Kolitsch A., Grötzschel R., Kierzek J.: Wettability improvement of carbon ceramic materials by mono and multi energy

plasma pulses, *Surface & Coatings Technology*, 2009, 203, 2536 - 2540

[11] Goki Eda, Manish Chhowalla: Graphene-based Composite thin films for electronics, *Nono Letters*, 2009, 9, 2, 814 - 818

[12] Stankovich S. et al.: Graphene based composite materials, *Nature Letters*, 2002, 442/20

[13] Strąk C., Siedlec R.: Lutowanie kompozytów miedź – grafen z ceramiką korundową za pomocą lutów aktywnych, *Materiały Elektroniczne*, 2014, 42, 4, 4 - 15

[14] Feng L. C., Shao W. Z., Zhen L., Xie N., Microstructure and mechanical property of Cu_2O-Cu cemet prepared by in-situ reduction-hot pressing method, *Science Direct, Material Letters,* 2008, 62, 3121 - 3123

[15] Xian Luo, Yanqing Yang, Cuixia Liu, Ting Xu, Meini Yuan and Bin Huang, The thermal expansion behavior of unidirectional SiC fiber-reinforced Cu–matrix composites, *Scripta Materialia*, 2008, 58, 401 - 404